Calculation of Drift Distortion Due to Imperfections in a TPC Cylindrical Field Cage

H. Wieman

Lawrence Berkeley National Laboratory

Abstract

We derive a formula for the radial drift distortion using a solution to Laplace's equation for the standard solenoidal TPC (Time Projection Chamber) field cage design with two concentric cylinders with closed ends. The calculation method is applied to the STAR TPC to study a variety of possible defects. One real defect caused by reduced insulator resistance is also examined. The distortion induced by measured errors in this case is shown to be within the allowed distortion tolerance. We also study the effects of finite stripe width, random resistor chain error, shorted equipotential rings and potential mismatch at the end cap surface. The calculation method that we have developed works for rotationally symmetric errors in the potential along either the inner or outer filed cage cylindrical walls. This document is written in Mathcad+6.0 and is available as a program for calculating other drift distortion problems.

1. Introduction

In a TPC the momentum resolution depends on the spacial resolution which in turn depends directly on the precision with which electrons drift through the gas in the electric field generated by the field cage. The errors in the electron drift path must be well under a mm for drift lengths on the order of 2 m. This imposes stringent limits on the field cage design and construction and requires calculations relating errors in the potential on the field cage surface to distortions in the electron drift path. The standard cylindrical TPC field cage, shown in Figure 1, is composed of two concentric cylinders closed at both ends with planes at right angles to the axis. A uniform field in the z direction is generated by linearly grading the potential from one end to the other with equipotential rings spaced uniformly along the inner and outer cylinder. Errors in the grading of the potential or in matching the potential on the cylinder with the end caps generate a radial component in the E field which causes a radial distortion in the electron drift path. More importantly, the radial E field causes a distortion in the azimuthal direction through the EXB term in the electron drift velocity. This azimuthal distortion to the drift path affects the sagitta measurement, thus limiting the momentum resolution. The types of errors of concern are those in the resistor chain coupling the grading rings or in reduced resistance in the field cage insulator, which has the same effect. The particular example calculated in this document addresses a measured reduced resistance in one of the insulating structures in the STAR TPC field cage.

The calculation and program presented here provide a quick and convenient method for determining the radial distortion from errors in the potential of the type just described. The examples that appear in this document required only a few seconds to calculate on a 90 MHz Pentium processor.

Our general approach, which works with an arbitrary rotationally symmetric error potential, expands on the method used by Blum and Rolandi [1] for calculating distortions that occur with a single cylinder geometry.

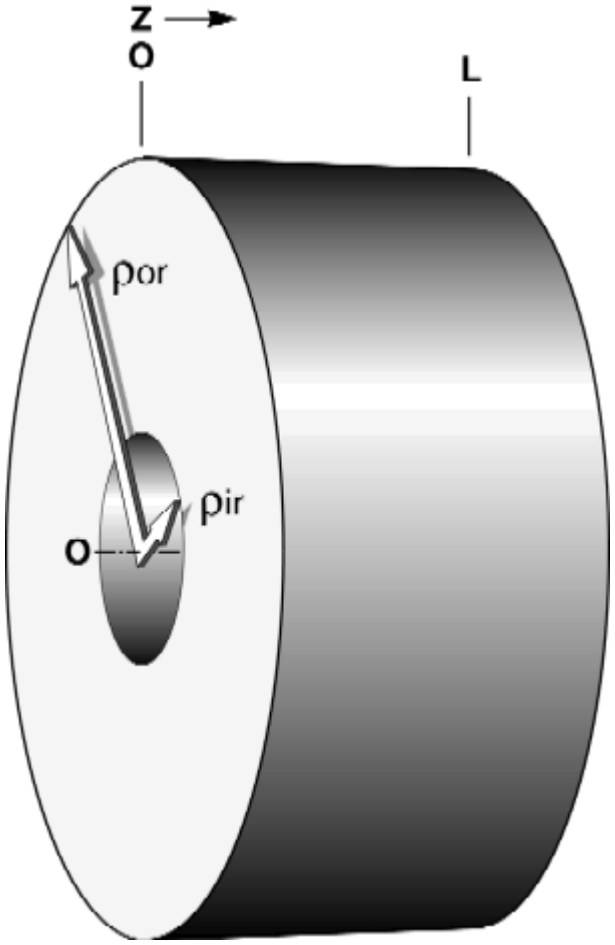

Figure 1. Diagram of the field cage geometry. The electrons drift parallel to the z axis and arrive at the read out plane on the end at z = 0. The electrons drift varying distances depending on their point of origin and have a maximum possible drift length of L. The potential is 0 at the z = 0 end and the end plate at z = L has a potential of V. The potential is graded along the inner cylinder at $\rho = \rho ir$ and the outer cylinder at $\rho = \rho or$. In this note we calculate the effects of deviation from a perfect linear boundary condition along the cylinder walls.

2. Method for Determining Drift Distortion

In calculating the drift distortion we assume that the distortion is relatively small so that we can integrate along a straight path and also ignore errors in E_z, the field component in the normal drift direction. With this caveat the deviation in the electron path in both the ρ and the azimuthal direction is proportional to the following integral[2] (Radial Distortion Integral, RDI):

$$\Delta\rho(\rho,z) = \int_z^0 \frac{E_\rho(\rho,z)}{E_z}\,dz \qquad (1)$$

where the integration starts at z, the point of electron creation, and stops at the end of the cylinder, z =0. In the absence of a magnetic field the deviation from a straight path parallel to the z axis is equal to $\Delta\rho$ of Eq. 1. and is directed radially in the ρ direction. For the normal case with a magnetic field parallel to the z axis the drift distortion has a component in the ρ direction which is

$$\delta\rho = \frac{1}{\left[1 + (\omega\cdot\tau)^2\right]}\cdot\Delta\rho \qquad (2)$$

and a component in the azimuthal direction

$$\delta\rho\phi = \frac{\omega\cdot\tau}{\left[1 + (\omega\cdot\tau)^2\right]}\cdot\Delta\rho \qquad (3)$$

that comes from the EXB term in the drift velocity expression. In the STAR experiment with a drift gas mixture of 10% CH_4 + 90% Ar and a magnetic field of 0.5 Tesla $\omega\tau$ = 3.

To evaluate the line integral we can solve Laplace's equation using just the error potential on the boundary conditions. The full drift field potential does not have to be included since potentials and fields are additive. The Bessel-Fourier expansion solution (see Appendix 1 for the derivation) is

$$\Delta\rho(\rho,z) = L\cdot\sum_{n=1}^{\infty}\left(a_n\cdot I1\left(\frac{n\cdot\pi\cdot\rho}{L}\right) - b_n\cdot K1\left(\frac{n\cdot\pi\cdot\rho}{L}\right)\right)\cdot\left(\cos\left(\frac{n\cdot\pi\cdot z}{L}\right) - 1\right) \qquad (4)$$

where the terms

$I1\left(\frac{n\cdot\pi\cdot\rho}{L}\right)$ and $K1\left(\frac{n\cdot\pi\cdot\rho}{L}\right)$ are modified Bessel functions of the first and second kind.

The coefficients a_n and b_n are obtained from the error potential boundary conditions as shown in the following expressions.

$$a_n = \frac{sir_n\cdot K0\left(\frac{n\cdot\pi\cdot\rho or}{L}\right) - sor_n\cdot K0\left(\frac{n\cdot\pi\cdot\rho ir}{L}\right)}{I0\left(\frac{n\cdot\pi\cdot\rho ir}{L}\right)\cdot K0\left(\frac{n\cdot\pi\cdot\rho or}{L}\right) - I0\left(\frac{n\cdot\pi\cdot\rho or}{L}\right)\cdot K0\left(\frac{n\cdot\pi\cdot\rho ir}{L}\right)} \qquad (5)$$

$$b_n = \frac{sor_n \cdot I0\left(\frac{n\cdot\pi\cdot\rho ir}{L}\right) - sir_n \cdot I0\left(\frac{n\cdot\pi\cdot\rho or}{L}\right)}{I0\left(\frac{n\cdot\pi\cdot\rho ir}{L}\right)\cdot K0\left(\frac{n\cdot\pi\cdot\rho or}{L}\right) - I0\left(\frac{n\cdot\pi\cdot\rho or}{L}\right)\cdot K0\left(\frac{n\cdot\pi\cdot\rho ir}{L}\right)} \qquad (6)$$

Where sir_n and sor_n are the following integrals along the inner and outer boundary cylinders

$$sir_n = \frac{2}{L}\cdot\int_0^L \phi(\rho ir, z)\cdot\sin\left(\frac{n\cdot\pi\cdot z}{L}\right) dz \qquad (7)$$

$$sor_n = \frac{2}{L}\cdot\int_0^L \phi(\rho or, z)\cdot\sin\left(\frac{n\cdot\pi\cdot z}{L}\right) dz \qquad (8)$$

with normalized error potentials

$$\phi(\rho ir, z) = \frac{\Phi(\rho ir, z)}{V} \quad \text{and} \quad \phi(\rho or, z) = \frac{\Phi(\rho or, z)}{V}$$

V is the drift voltage on the z = L end plate of the field cage.

The error potential solution in the volume which was used to get the distortion integral is

$$\Phi(\rho, z) = V\cdot\sum_{n=1}^{\infty}\left(a_n\cdot I0\left(\frac{n\cdot\pi\cdot\rho}{L}\right) + b_n\cdot K0\left(\frac{n\cdot\pi\cdot\rho}{L}\right)\right)\cdot\sin\left(\frac{n\cdot\pi\cdot z}{L}\right) \qquad (9)$$

The number of terms required in the sum, Eq. 4, to accurately calculate the distortion integral depends on the spacial frequency of the error potential on the boundary. We use the potential expression , Eq. 9, to check the number of terms required to give a reasonable approximation of the input error potential boundary conditions.

3. Drift Distortion in the STAR Field Cage from Reduced Insulator Resistance

During construction of the STAR TPC field cage we have found a region of reduced resistance caused by a particular application of epoxy on the outer field cage structure. The method developed above is used to evaluate the distortion that will result. The resistance has been measured between the equipotential stripes by biasing adjacent stripes with 500 volts and measuring the current. The measured resistance in parallel with the planed resistor chain value of 2 M Ω per stripe is used to calculate the error potential. Figure 2 shows the resulting parallel resistance which at the low z end of the cylinder is below the optimum value of 2 MΩ

$kk := 0 .. Nk - 1$

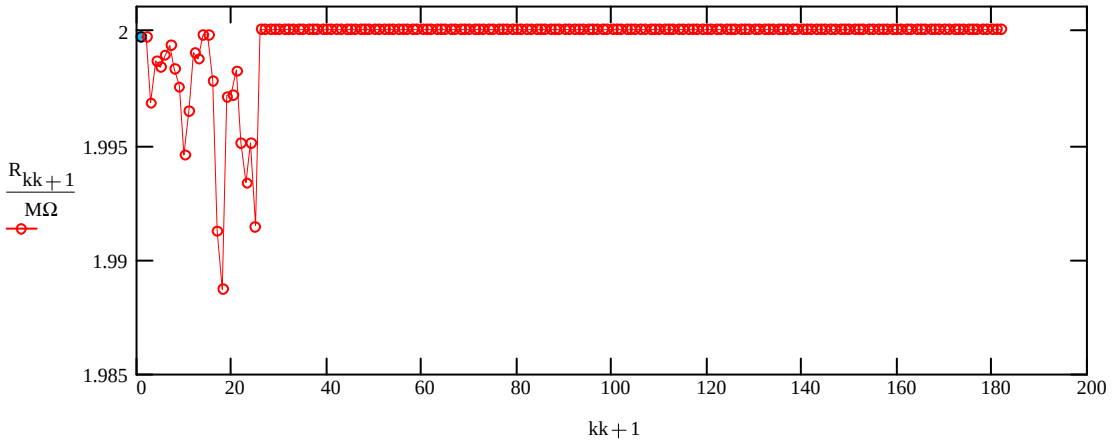

Figure 2. Resistance between stripes with the 2 MΩ resistors of the resistor chain plus the parallel resistance through the epoxy.

Field cage dimensions to be used in the calculation

$L := 210 \cdot cm$ length of the field cage cylinder

$\rho or := 200 \cdot cm$ outer cylinder radius

$\rho ir := 50 \cdot cm$ inner cylinder radius

Using the stripe to stripe resistance find the error potential

$RT := \sum_{k} R_k$ Total field cage resistance

$RS_0 := 0 \cdot \Omega$

$RS_{kk+1} := RS_{kk} + R_{kk+1}$ running sum of resistance is proportional to potential at each equipotential ring (stripe)

$\frac{RS_k}{RT}$ normalized true potential on each ring of the outer field cage

$\frac{k}{Nk}$ normalized ideal potential

$Scf := 10^4$ scaling factor to improve accuracy of numerical calculations

$\phi or_k := Scf \cdot \left(\frac{RS_k}{RT} - \frac{k}{Nk} \right)$ normalized error potential boundary condition with a scaling factor

$zs_k := k \cdot \frac{L}{Nk}$ z location of each stripe

$\phi orc(z) := linterp(zs, \phi or, z)$ boundary error potential as a continuous function for use in integration

$Nn := 20$ number of terms to carry in the expansion

$n := 1 .. Nn$

$sor_n := \frac{2}{L} \cdot \int_0^L \phi orc(z) \cdot \sin\left(\frac{n \cdot \pi \cdot z}{L} \right) dz$ integration along outer field cage cylinder as in Eq. 8

$sir_n := 0$ in this example the error boundary potential on the inner field cage is assumed to be 0

$$a_n := \frac{sir_n \cdot K0\left(\frac{n \cdot \pi \cdot \rho or}{L}\right) - sor_n \cdot K0\left(\frac{n \cdot \pi \cdot \rho ir}{L}\right)}{I0\left(\frac{n \cdot \pi \cdot \rho ir}{L}\right) \cdot K0\left(\frac{n \cdot \pi \cdot \rho or}{L}\right) - I0\left(\frac{n \cdot \pi \cdot \rho or}{L}\right) \cdot K0\left(\frac{n \cdot \pi \cdot \rho ir}{L}\right)}$$

using Eq. 5 and Eq. 6

$$b_n := \frac{sor_n \cdot I0\left(\frac{n\cdot\pi\cdot\rho ir}{L}\right) - sir_n \cdot I0\left(\frac{n\cdot\pi\cdot\rho or}{L}\right)}{I0\left(\frac{n\cdot\pi\cdot\rho ir}{L}\right)\cdot K0\left(\frac{n\cdot\pi\cdot\rho or}{L}\right) - I0\left(\frac{n\cdot\pi\cdot\rho or}{L}\right)\cdot K0\left(\frac{n\cdot\pi\cdot\rho ir}{L}\right)}$$

using Eq. 9 to check the coefficients to see that the boundary conditions are reproduced

$$\phi(\rho,z) := \frac{1}{Scf}\cdot\sum_n\left(a_n\cdot I0\left(\frac{n\cdot\pi\cdot\rho}{L}\right) + b_n\cdot K0\left(\frac{n\cdot\pi\cdot\rho}{L}\right)\right)\cdot\sin\left(\frac{n\cdot\pi\cdot z}{L}\right) \qquad (10)$$

$$\phi cir_k := \phi\left(\rho ir, zs_k\right)$$

$$\phi cor_k := \phi\left(\rho or, zs_k\right)$$

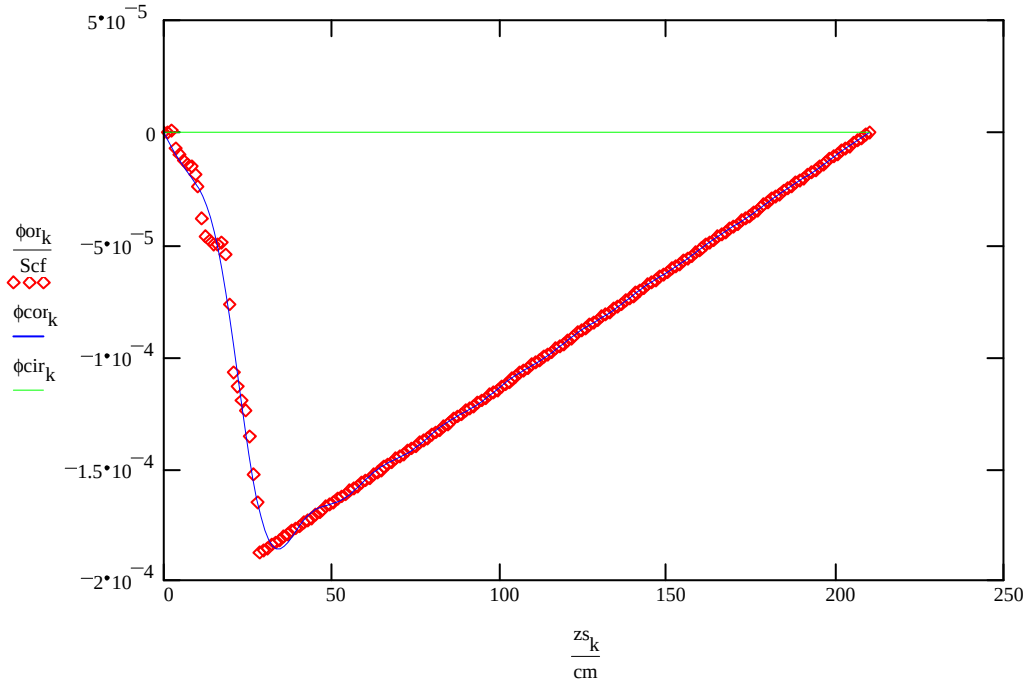

Figure 3. The red diamonds show the input error potential boundary conditions on the outer field cage along the full length of the field cage. The blue line shows the reconstructed error potential on the outer field cage using the solution to Laplace's equation. The green line shows the reconstructed boundary condition on the inner field cage cylinder which is 0.

As shown in Figure 3 the solution gives a reasonably good reproduction of the starting boundary conditions with 20 terms in the summation. Having verified the solution we calculate the distortion integral using Eq. 4 and plot the distortion integral for the full drift length as a function of radius.

$$\Delta\rho(\rho,z) := L\cdot\frac{1}{Scf}\cdot\sum_{n}\left(a_n\cdot I1\left(\frac{n\cdot\pi\cdot\rho}{L}\right) - b_n\cdot K1\left(\frac{n\cdot\pi\cdot\rho}{L}\right)\right)\cdot\left(\cos\left(\frac{n\cdot\pi\cdot z}{L}\right) - 1\right)$$

$Nk := 40$

$k := 0 .. Nk$

$\Delta r := \frac{\rho or - \rho ir}{Nk}$

$\rho_k := \Delta r\cdot k + \rho ir$

$\rho m_k := \Delta\rho\left(\rho_k, 200\cdot cm\right)$

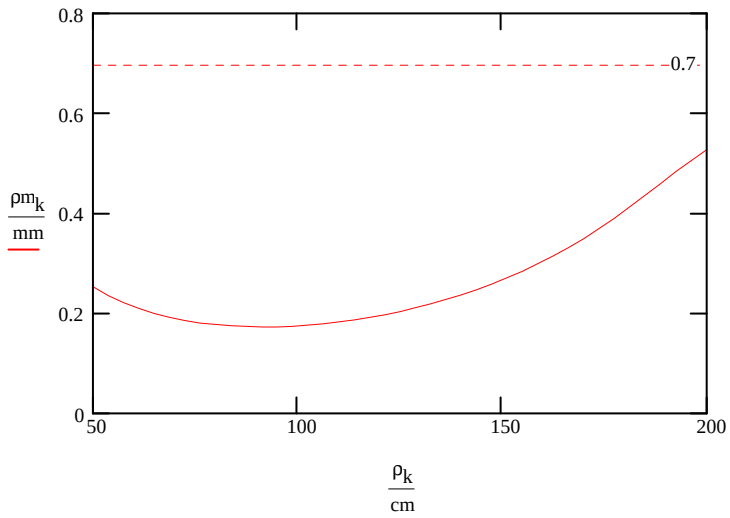

Figure 4. The radial distortion integral is shown for the full drift length as a function of radius. Note that the error is not a minimum at the inner field cage even though the potential error in this example is only on the outer field cage. The maximum allowed value, 0.7 mm, for the distortion integral is shown on the plot for comparison.

The curve in Figure 4 will generate a false sagitta when it is coupled into the azimuthal direction. Using Eq. 2 and $\omega\tau$ = 3 we get a false sagitta value of 60 μm.

The following prepares a plot of the distortion integral as a function of z for 4 values of ρ

$Nm := 80$

$m := 0 .. Nm$

$$\rho := \begin{bmatrix} 195 \\ 190 \\ 180 \\ 160 \end{bmatrix} \cdot cm$$

$k := 0 .. last(\rho)$

$$z_m := \frac{L}{Nm} \cdot m$$

$\delta\rho a_{k,m} := \Delta\rho\left(\rho_k, z_m\right)$ $\rho m_k := \Delta\rho\left(\rho_k, 200 \cdot cm\right)$

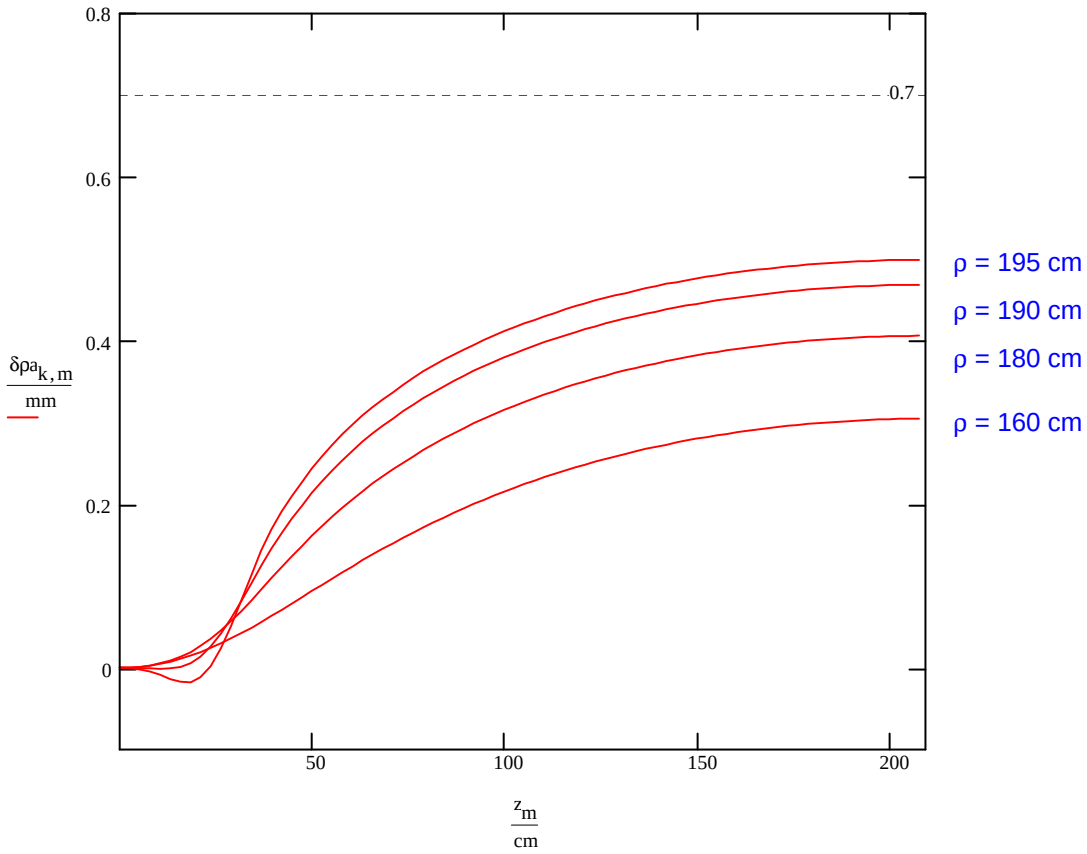

Figure 5. The distortion integral is plotted as a function of z, the electron starting point, at four different radius values. The largest distortion shown is for a radius that is 5 cm from the outer field cage cylinder.

Preparation for a similar plot for radii closer to the inner field cage cylinder

$$\rho := \begin{bmatrix} 55 \\ 60 \\ 70 \\ 90 \end{bmatrix} \cdot cm$$

$$\delta\rho a_{k,m} := \Delta\rho\left(\rho_k, z_m\right)$$

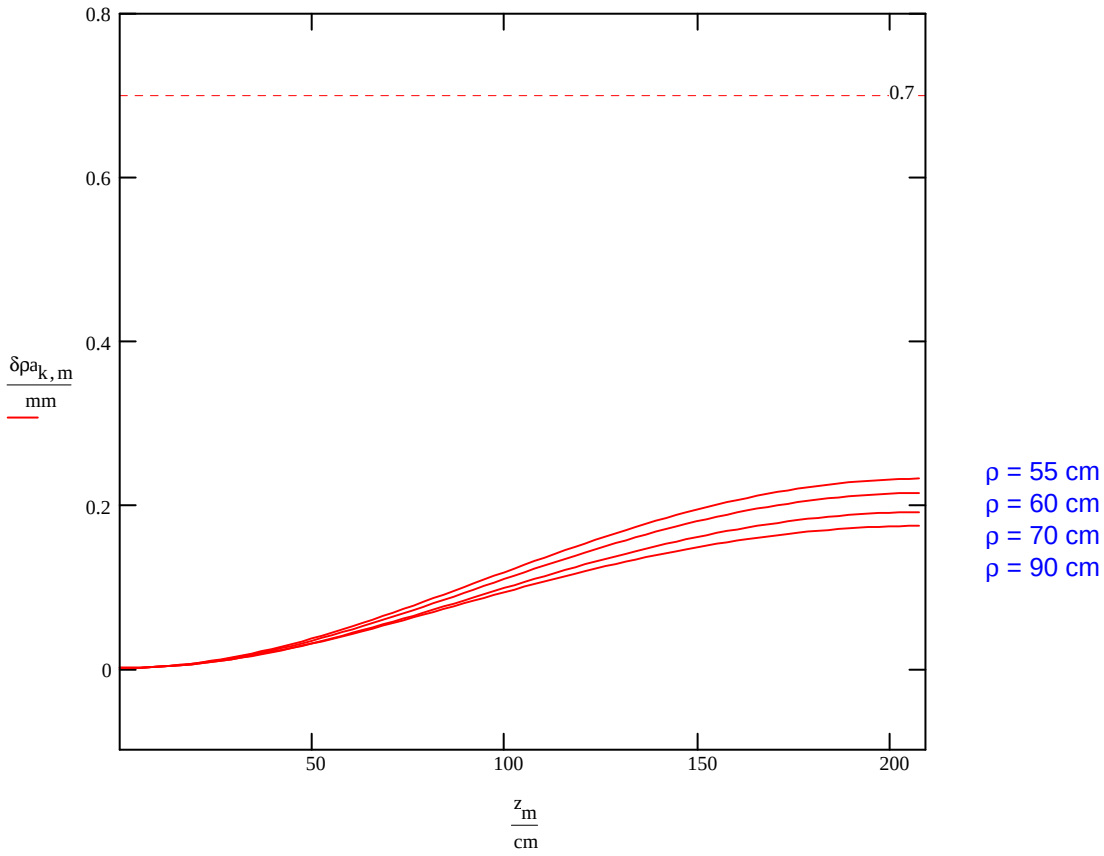

Figure 6. The distortion integral is plotted as a function of z, the electron starting point, at four different radius values closer to the inner field cage radius. Again the largest distortion occurs for the radii close to the field cage boundary.

It has been shown that the reduced resistance in a section of the field cage with some parallel resistances as low as 100 times the nominal resistor chain value causes some error, but the error is well within the design tolerance of 0.7 mm for the radial distortion integral.

4. Radial Distortion from Finite Width Equipotential Stripes

The field cage cylinder is constructed with uniform width (1 cm wide) copper stripes that are separated with as small a gap as can be safely used to hold off the potential difference between the stripes. This step-wise grading of the potential deviates from the ideal case with a uniform continuous grading. It is well known that the error caused by this construction is extremely small at distances from the field cage wall that are a few times the band width, but we can in principle apply our method to get a good quantitative value for the distortion. The results show that we can safely join stripes, effectively increasing the stripe width as long as the center potentials of all the stripes are correctly maintained. This is useful knowledge since it simplifies the construction of the support for the central membrane.

To define the boundary conditions for this problem we assume that the uniform stripes are touching and the ends of the cylinder intersect the centers of the end stripes. The center of the stripes are at the correct potential and the error potential increases linearly with the z distance from the stripe center. The solution is as follows.

$L := 200 \cdot cm$ cylinder length in round numbers for convenience

$Ns := 20$ number of uniform bands or stripes that the cylinder is divided into

$ns := 5$

$w := \frac{L}{Ns}$ $w = 10 \cdot cm$ width of a stripe

$Nn := ns \cdot 2 \cdot Ns$ selected number of terms in the Fourier expansion

The integrals (Eqs. 7 and 8, the same in this case) can be evaluated analytically and are 0 for many values of n. The result is:

$n := 2 \cdot Ns, 4 \cdot Ns .. Nn$

$sir_n := \frac{2}{n \cdot \pi} \cdot (-1)^{\frac{n}{2 \cdot Ns}}$

$sor := sir$

The coefficients are given as before by Eqs. 5 and 6

$$a_n := \frac{sir_n \cdot K0\left(\frac{n \cdot \pi \cdot \rho or}{L}\right) - sor_n \cdot K0\left(\frac{n \cdot \pi \cdot \rho ir}{L}\right)}{I0\left(\frac{n \cdot \pi \cdot \rho ir}{L}\right) \cdot K0\left(\frac{n \cdot \pi \cdot \rho or}{L}\right) - I0\left(\frac{n \cdot \pi \cdot \rho or}{L}\right) \cdot K0\left(\frac{n \cdot \pi \cdot \rho ir}{L}\right)}$$

$$b_n := \frac{sor_n \cdot I0\left(\frac{n \cdot \pi \cdot \rho ir}{L}\right) - sir_n \cdot I0\left(\frac{n \cdot \pi \cdot \rho or}{L}\right)}{I0\left(\frac{n \cdot \pi \cdot \rho ir}{L}\right) \cdot K0\left(\frac{n \cdot \pi \cdot \rho or}{L}\right) - I0\left(\frac{n \cdot \pi \cdot \rho or}{L}\right) \cdot K0\left(\frac{n \cdot \pi \cdot \rho ir}{L}\right)}$$

and, by Eq. 10, the normalized error potential is

$$\phi(\rho,z) := \sum_n \left(a_n \cdot I0\left(\frac{n\cdot\pi\cdot\rho}{L}\right) + b_n \cdot K0\left(\frac{n\cdot\pi\cdot\rho}{L}\right)\right)\cdot\sin\left(\frac{n\cdot\pi\cdot z}{L}\right)$$

We plot the resulting potential solution above on the boundaries to compare with the specified boundary conditions.

$Nk := 800$

$k := 0 .. Nk$

$\delta z := \frac{L}{Nk\cdot 5}$

$z_k := k\cdot\delta z$

$\varepsilon d := .0008$

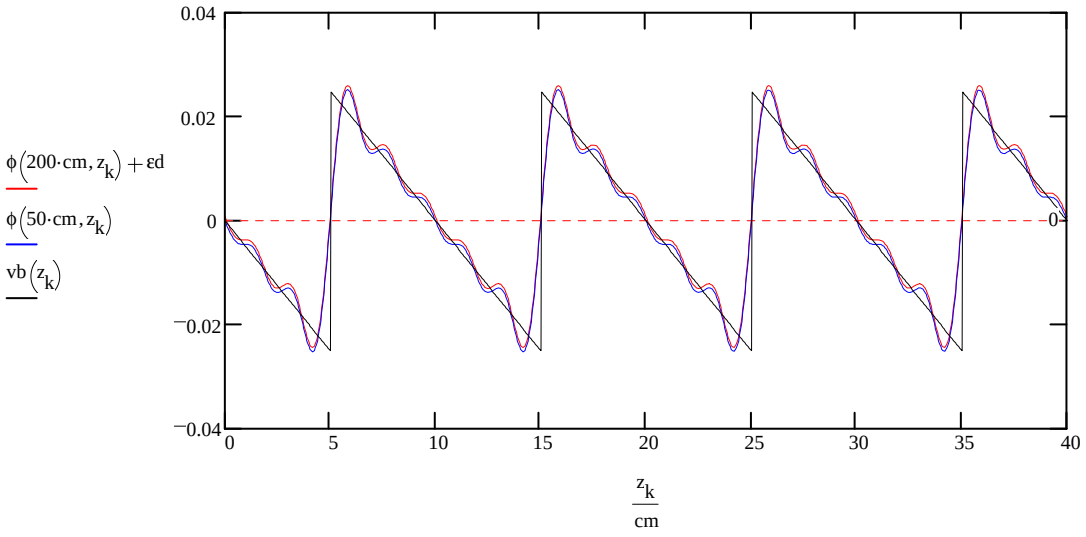

Figure 7. The generated potential solution is shown on the inner and outer cylinder boundaries. The solution for the outer cylinder (in red) has been displaced slightly since it would otherwise overlap completely with the solution at the inner cylinder. The specified error potential for finite width stripes used to generate the solution is shown in black. The reconstructed potential is close, but not perfect due to the limited number of terms in the expansion. In the interest of clarity only 1/5 of the 200 cm cylinder is shown here.

Again using Eq. 4 the distortion integral is:

$$\Delta\rho(\rho,z) := L\cdot\sum_{n}\left(a_n\cdot I1\left(\frac{n\cdot\pi\cdot\rho}{L}\right) - b_n\cdot K1\left(\frac{n\cdot\pi\cdot\rho}{L}\right)\right)\cdot\left(\cos\left(\frac{n\cdot\pi\cdot z}{L}\right) - 1\right)$$

which is shown in Figure 8 plotted as a function of z for paths 5 cm from the inner and outer field cage cylinders.

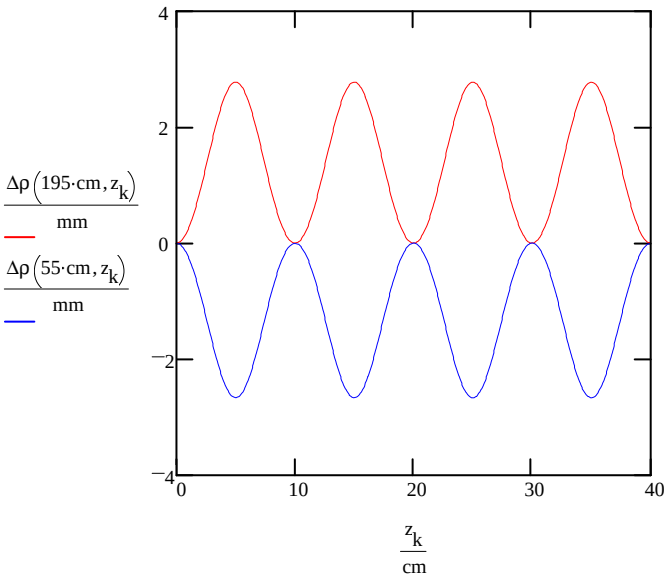

Figure 8. The radial distortion integral is shown along part of the field cage wall. The red curve is the distortion 5 cm from the outer field cage boundary and the blue curve in the distortion 5 cm from the inner field cage boundary. Electron paths that originate with z values centered on the stripes would end up with zero distortion and paths starting at the junction between stripes get the maximum distortion. The sign of the distortion is always such that the point of origin will appear to be closer to the near cylinder wall.

$Ni := 80$

$i := 0 .. Ni$

The radial dependence of the distortion is shown in the next plot (Figure 9). For this plot a z value is chosen to maximize the distortion.

$$r_i := \rho ir + i\cdot\frac{\rho or - \rho ir}{Ni}$$

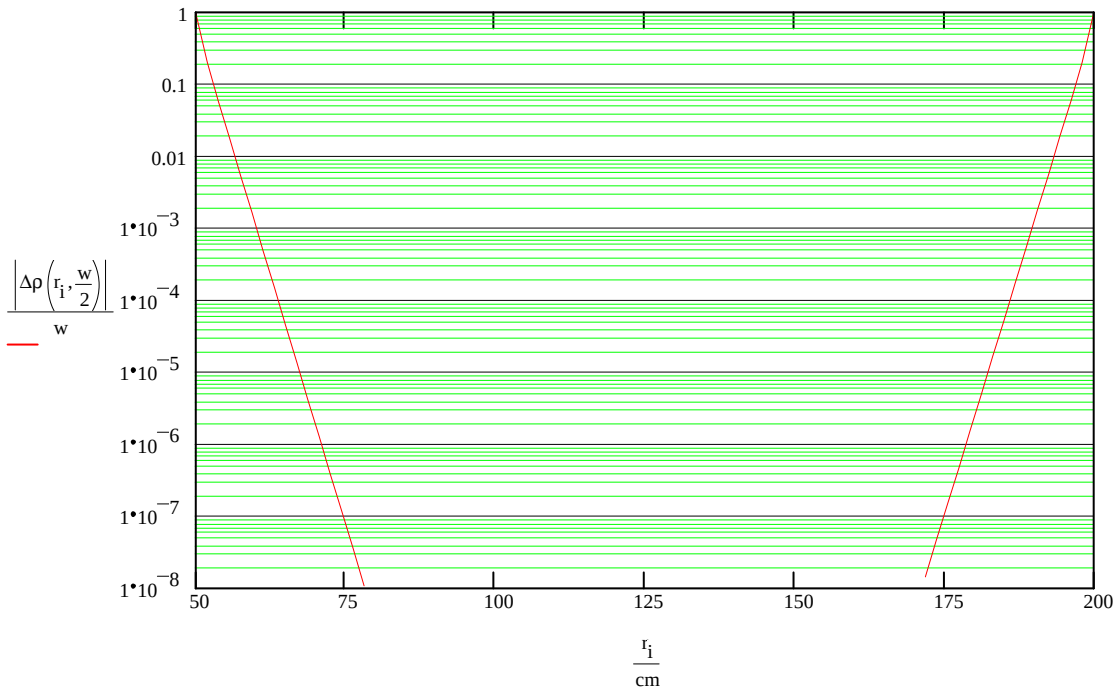

Figure 9. The magnitude of the radial distortion integral divided by the stripe width is shown as a function of radius. As expected the distortion heals rapidly as one moves away from the field cage walls.

The example shown in Figs. 8 and 9 is for 10 cm wide stripes, a value that is roughly 10 times the width of the stripes in the STAR field cage. In principle this approach could be applied to smaller stripes, but in practice we are limited by the size of the Bessel function arguments. For large arguments the Bessel functions go as exponentials of the arguments and overflow results. By choosing different sized stripes we have found that the amplitude scales approximately as shown in Eq. 11 below.

$$\Delta\rho(x,w) := w\cdot\exp\left[-\left(\frac{x}{w}\right)\cdot\ln(1000)\right] \qquad (11)$$

where

w is the stripe width and

x is the distance from the field cage wall

For the STAR TPC w is 1.1 cm and the field cage wall is more than 5 cm from the useful tracking region so the distortion from this effect is less than

$$\Delta\rho(5\cdot cm, 1.1\cdot cm) = 2.5\cdot 10^{-10}\ \cdot\mu m$$

This result shows that we can safely join stripes if necessary to facilitate construction of the central membrane support. Joining 2 stripes on either side of the center stripe is equivalent to increasing the stripe width by 5. In this case the distortion amplitude is

$\Delta\rho(5\cdot cm, 5.5\cdot cm) = 103\cdot\mu m$ which is well below our 700 μm limit.

5. Distortions from Random Resistor Errors in the Resistor Chain

In order to determine the precision required for the resistors in the field cage resistor chain we have calculated the radial distortion integral for a field cage where the resistors have been assigned random values within specified limits. The calculation of the radial distortion integral has been performed in the same manner as was done in section 3. In this Monte Carlo exercise the resistor values have been given a uniform random value between +- 0.2 %. This is equivalent to an rms resistor error of 0.12 %. A typical error potential for the inner and outer cylinder boundary condition is shown in Figure 10 along with Fourier expansion of the boundary potential used to find the radial distortion integral. The number of a and b coefficients in the expansion is

$Nn = 40$

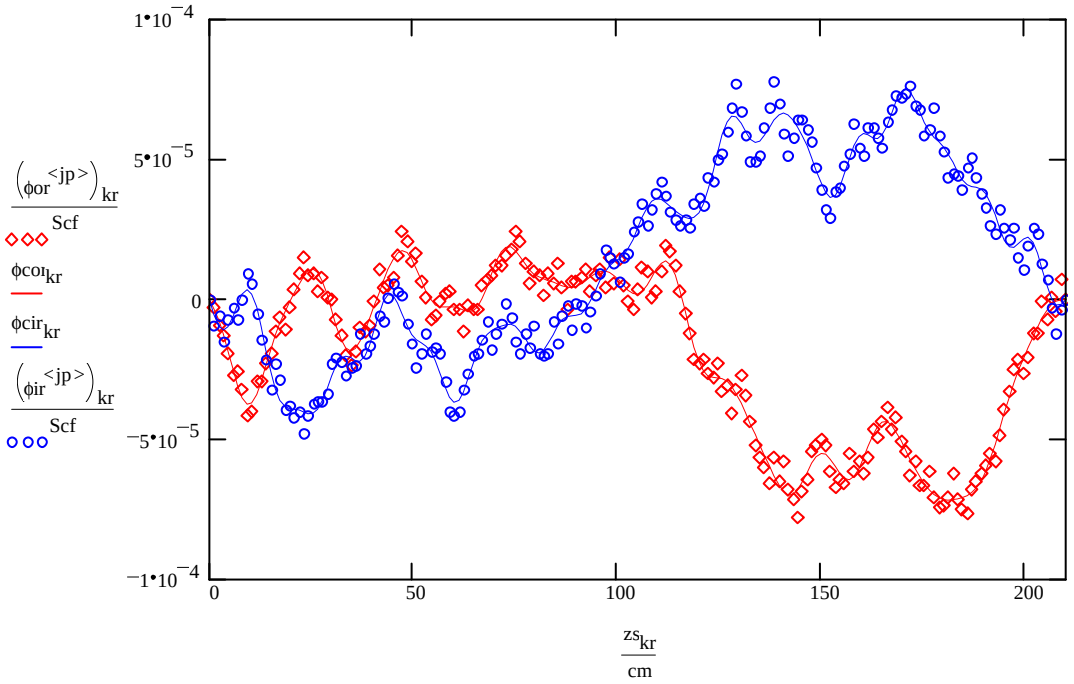

Figure 10. The points show a typical normalized error potential for each equipotential stripe of the field cage where the resistors in the resistor chain have been assigned a random value between +- 0.2 % of the nominal value. The blue circles show the error potential on the inner cylinder and the red diamonds show the error potential on the outer cylinder. The smooth curves show the expansion representation of the error potential.

The radial distortion integrals 5 cm from the inner and outer field cage cylinder are shown below in Figure 11 for two example cases.

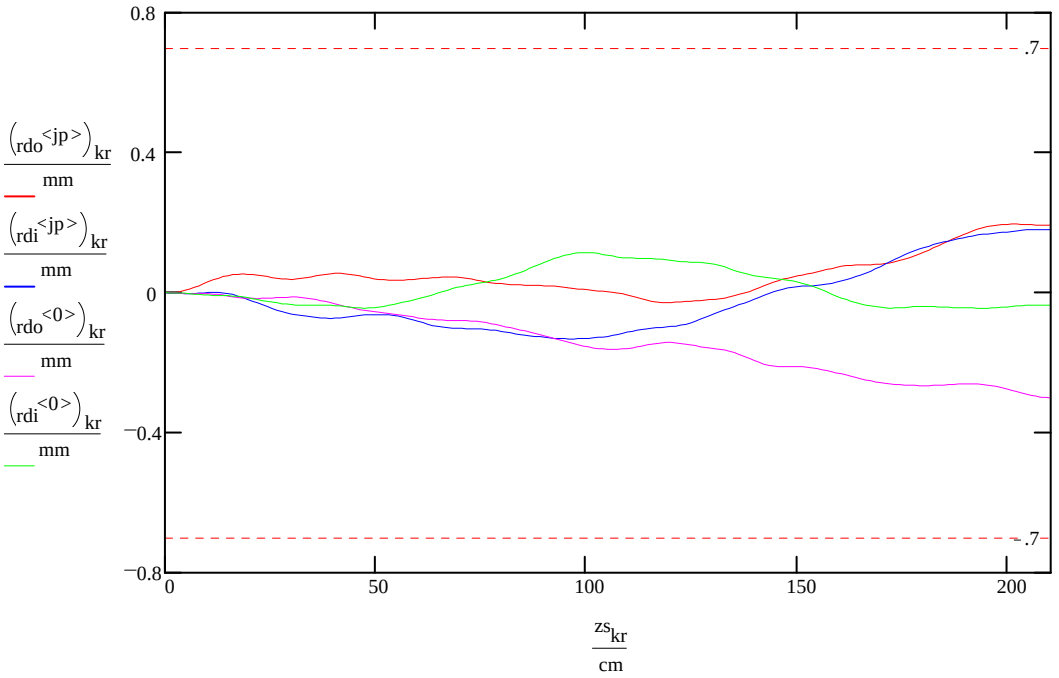

Figure 11. Two example cases of the radial distortion integrals are shown as a function of drift distance along z. The red and magenta curves are for the path 5 cm from the outer field cage cylinder and the blue and green curves are for the path 5 cm from the inner field cage cylinder. The red and blue curves are for the same case with error potentials given in Figure 10. In both cases the resistors in the resistor chain vary randomly between +- 0.2 %. The limits on acceptable distortion are show at + an - 0.7 mm.

Just two examples are shown in Figure 11. We have run 60 cases and histogramed the maximum amplitudes of the radial distortion integral in Figure 12.

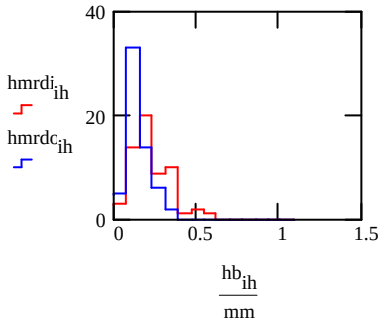

Figure 12. Histogram of the maxima in the radial distortion integral for different resistor runs. As before the resistors vary randomly between +- 0.2% of nominal. The red curve is for the path 5 cm from the inner cylinder and the blue curve is for the path 5 cm from the outer cylinder.

As shown in Figure 12 there is considerable variation in the distortion for a given selection of resistor precision. The magnitude of the distortion depends strongly on the ordering of the resistor selection. We show two different orderings of the same resistor set. In one case the resistors are ordered in ascending order starting with the lower values at z = 0. In the other case we pair-wise order the resistors with, the larger resistors placed next to the smallest resistors. The error potentials for the two sorting conditions are shown in Figure 13 and the resulting radial distortion integrals are shown in Figure 14.

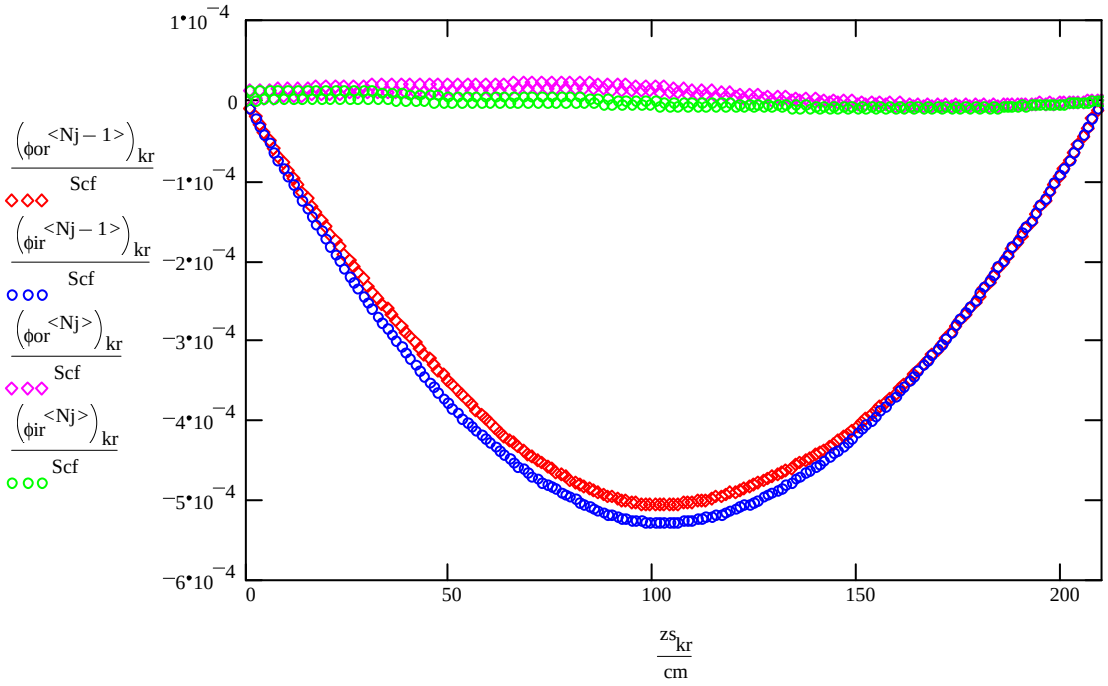

Figure 13. The error potential on the inner and outer cylinder boundaries for two different sortings of the resistors in the resistor chain. The large error (red points outer cylinder and blue points inner cylinder) results from sorting the resistors in increasing resistance from z = 0 to z = 210. The magenta points (outer cylinder) and green points (inner cylinder) show the error potential for resistors sorted with the largest and smallest values paired starting from z = 0 and progressing with less divergent pairs to z = 210.

The distortion results in Figure 14 show that, even with resistors that have been limited to a reasonably tight tolerance (+- 0.2 %), the ordering of the resistor values can have a significant effect on the distortion. When the resistors are sorted with values increasing with z the error is 2 to 3 times the allowed value of 0.7 mm. The error is much smaller when the largest resistors are paired adjacent to the resistors with the smallest values. This shows that a potential error between two stripes can be compensated by correcting on the next stripe pair. This pair-wise sorting, however, does not provide a significant improvement over the purely random distribution which is represented in Figure 12.

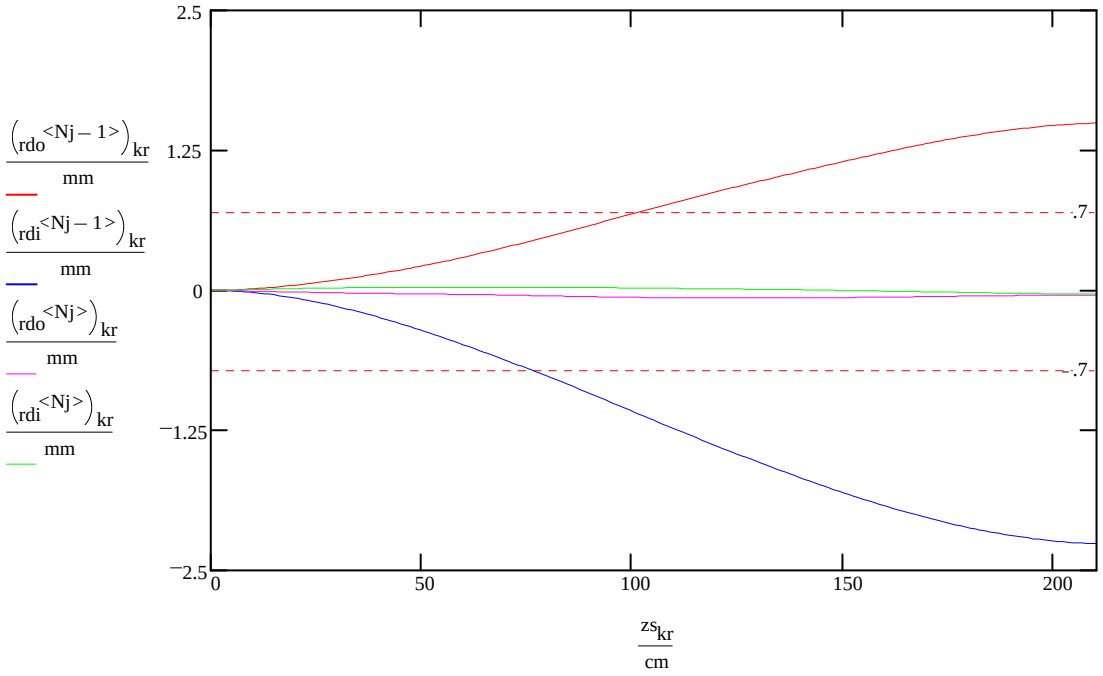

Figure 14. The radial distortion integral 5 cm from the inner and outer field cage cylinder plotted as a function of z for different sorting conditions on the resistors in the resistor chain. The red and blue curves show the distortion integral for resistors that have been sorted in increasing value from z = 0 to z = 210 cm. The red curve is the distortion next to the outer field cage cylinder and the blue curve is for the path next to the inner cylinder. The magenta and green curves (outer and inner cylinder paths respectively) are for the same resistors sorted pair-wise with the largest value next to the smallest value.

6. Distortion Caused by Shorted Stripes

The radial distortion integral is calculated for a condition where two stripes of the outer field cage cylinder are shorted together. The potential along the cylinder, Vz, can be represented as a continuous function of z, ignoring the discrete stripe nature of the cage.

$$Vz(z) = R(z)\cdot I \qquad \text{where} \qquad R(z) = \begin{cases} \frac{Rd}{\Delta z}\cdot z & z<zsh \\ \frac{Rd}{\Delta z}\cdot z - Rd & z>zsh \end{cases}$$

and

Δz stripe period

$Nr := 182$ number of resistors in the chain

$zsh := 158 \cdot cm$ short location in z

Rd individual resistor value in the chain

$I = \frac{V}{(Nr - 1) \cdot Rd}$ current in the shorted resistor chain

V total voltage on the field cage

Subtracting the ideal potential and normalizing to the total field cage voltage gives the normalized error potential.

$$\phi(z) = \begin{bmatrix} \frac{1}{L} \cdot \left(\frac{1}{Nr - 1} \right) \cdot z & z<zsh \\ \frac{1}{L} \cdot \left(\frac{1}{Nr - 1} \right) \cdot z - \frac{1}{Nr - 1} & z>zsh \end{bmatrix}$$

$Nn := 80$

$n := 1 .. Nn$

Substituting this expression for the error potential into Eq. 8 and performing the integration gives

$$sor_n := -2 \cdot \frac{\cos\left(n \cdot \pi \cdot \frac{zsh}{L} \right)}{(n \cdot \pi \cdot (Nr - 1))}$$

$sir_n := 0$

and again using Eqs. 5, 6 and 4

$$a_n := \frac{sir_n \cdot K0\left(\frac{n \cdot \pi \cdot \rho or}{L} \right) - sor_n \cdot K0\left(\frac{n \cdot \pi \cdot \rho ir}{L} \right)}{I0\left(\frac{n \cdot \pi \cdot \rho ir}{L} \right) \cdot K0\left(\frac{n \cdot \pi \cdot \rho or}{L} \right) - I0\left(\frac{n \cdot \pi \cdot \rho or}{L} \right) \cdot K0\left(\frac{n \cdot \pi \cdot \rho ir}{L} \right)}$$

$$b_n := \frac{sor_n \cdot I0\left(\frac{n \cdot \pi \cdot \rho ir}{L} \right) - sir_n \cdot I0\left(\frac{n \cdot \pi \cdot \rho or}{L} \right)}{I0\left(\frac{n \cdot \pi \cdot \rho ir}{L} \right) \cdot K0\left(\frac{n \cdot \pi \cdot \rho or}{L} \right) - I0\left(\frac{n \cdot \pi \cdot \rho or}{L} \right) \cdot K0\left(\frac{n \cdot \pi \cdot \rho ir}{L} \right)}$$

$$\Delta\rho(\rho,z) := L\cdot\sum_{n}\left(a_n\cdot I1\left(\frac{n\cdot\pi\cdot\rho}{L}\right) - b_n\cdot K1\left(\frac{n\cdot\pi\cdot\rho}{L}\right)\right)\cdot\left(\cos\left(\frac{n\cdot\pi\cdot z}{L}\right) - 1\right)$$

The radial distortion integral, $\Delta\rho(\rho,z)$, resulting from a shorted stripe on the outside cylinder is displayed for the full drift volume in Figure 15. The sign of the distortion is reversed in the figure for viewing. The radial distortion integral is everywhere negative, i.e. the distortion is toward the inner radius. Note that the distortion is a minimum around ρ = 95 cm and increases nearer the inner cylinder even though there is no potential error on the inner cylinder at ρ = 50 cm.

$dd := 5\cdot cm$ display grid size

$Nj := floor\left(\frac{L}{dd}\right)$ $Nk := floor\left(\frac{\rho or - \rho ir}{dd}\right)$

$j := 0..Nj$ $k := 0..Nk$

$zg_j := j\cdot dd$ $\rho g_k := \rho ir + dd\cdot k$

$$M\Phi_{j,k} := \frac{-\Delta\rho\left(\rho g_k, zg_j\right)}{mm}$$

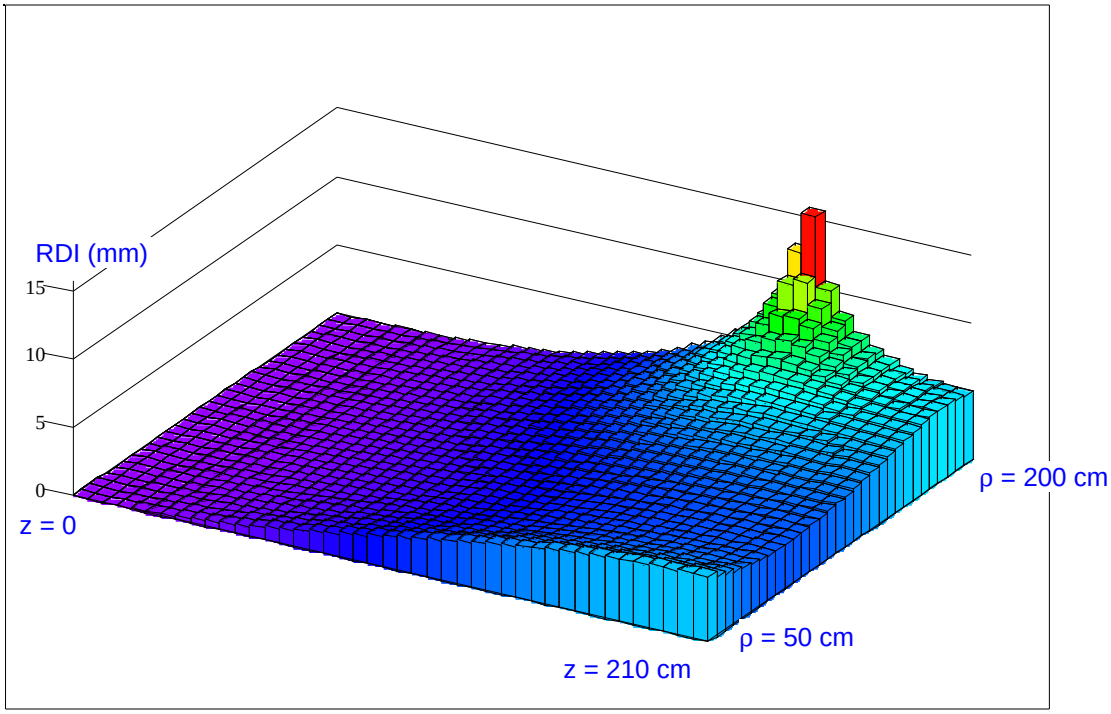

MΦ

Figure 15. Values of the radial distortion integral (sign reversed) in the full drift volume for a shorted stripe on the outer cylinder of the field cage 1/4 of the way from the central membrane.

The radial distortion integral is shown for specific selected radii in Figure 16. The inner radius displayed (95 cm) is near the minimum in the distortion and the outer radius shown (195 cm) is near the limit of used volume in the field cage.

$$Nm := 80$$

$$m := 0 .. Nm$$

$$z_m := \frac{L}{Nm} \cdot m$$

$$\rho := \begin{bmatrix} 195 \\ 190 \\ 180 \\ 160 \\ 95 \end{bmatrix} \cdot cm$$

$$k := 0 .. last(\rho)$$

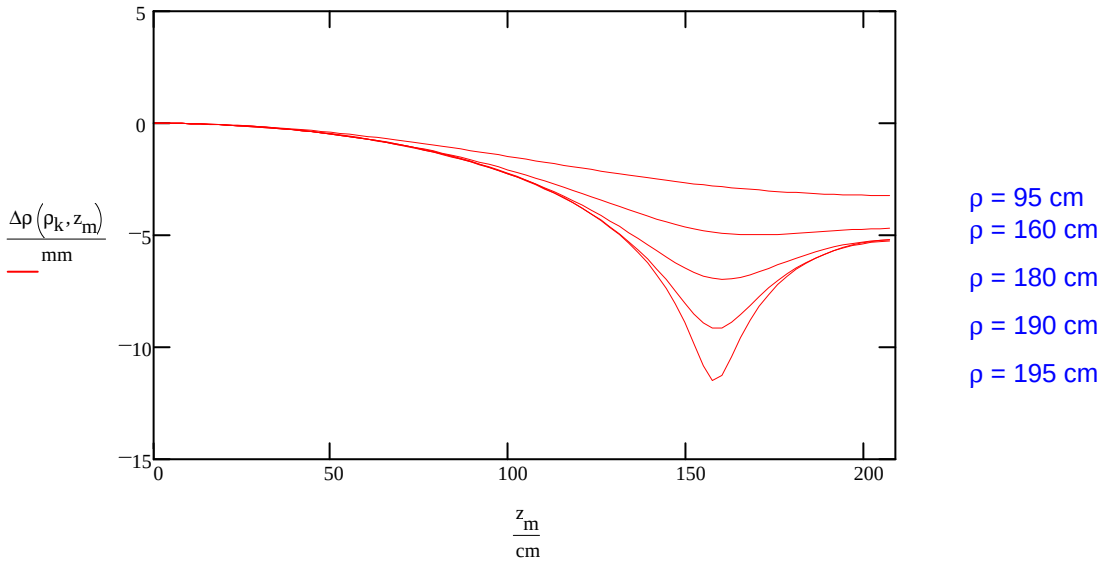

Figure 16. A plot of the radial distortion integral as a function of z for selected radii. The distortion is calculated for a pair of shorted stripes on the out field cage cylinder at z = 158 cm.

The distortion is over 1 cm in some places, greatly exceeding the design requirement of 0.7 mm.

7. Distortion from Potential Mismatch with the Cylinder Endcap

Distortions can arise from incorrect matching of the end cap potential with the field cage cylinder. This is most likely to happen at the ground end where the pad plane multi-wire proportional chambers define the potential. The effective position of the ground plane depends on the amount of field leakage from the anode wires and its compensation with the gating grid plane bias. The ground end of the field cage cylinder can be biased to achieve the correct matching. The following calculation shows the form of the distortion when this matching bias is incorrect.

We represent the mismatch with the endcap as the following error potential on the inner and outer cylinder boundaries[4].

$$\phi(z) = \delta V \cdot \frac{L - z}{L}$$

where δV is the potential mismatch at the endcap expressed as a fraction of the total potential on the field cage.

Using Eqs. 7 and 8 with the above error potential

$$sor_n = sir_n = \frac{2}{L} \cdot \int_0^L \delta V \cdot \frac{L - z}{L} \cdot \sin\left(\frac{n \cdot \pi \cdot z}{L}\right) dz$$

gives

$$sor_n = sir_n = \frac{2 \cdot \delta V}{n \cdot \pi}$$

choose $\delta V := 10^{-4}$

$$sor_n := \frac{2 \cdot \delta V}{n \cdot \pi} \qquad sir_n := \frac{2 \cdot \delta V}{n \cdot \pi}$$

and again using Eqs. 5, 6 and 4 to get the coefficients and the radial distortion integral

$$a_n := \frac{sir_n \cdot K0\left(\frac{n \cdot \pi \cdot \rho or}{L}\right) - sor_n \cdot K0\left(\frac{n \cdot \pi \cdot \rho ir}{L}\right)}{I0\left(\frac{n \cdot \pi \cdot \rho ir}{L}\right) \cdot K0\left(\frac{n \cdot \pi \cdot \rho or}{L}\right) - I0\left(\frac{n \cdot \pi \cdot \rho or}{L}\right) \cdot K0\left(\frac{n \cdot \pi \cdot \rho ir}{L}\right)}$$

$$b_n := \frac{sor_n \cdot I0\left(\frac{n \cdot \pi \cdot \rho ir}{L}\right) - sir_n \cdot I0\left(\frac{n \cdot \pi \cdot \rho or}{L}\right)}{I0\left(\frac{n \cdot \pi \cdot \rho ir}{L}\right) \cdot K0\left(\frac{n \cdot \pi \cdot \rho or}{L}\right) - I0\left(\frac{n \cdot \pi \cdot \rho or}{L}\right) \cdot K0\left(\frac{n \cdot \pi \cdot \rho ir}{L}\right)}$$

$$\Delta\rho(\rho, z) := L \cdot \sum_n \left(a_n \cdot I1\left(\frac{n \cdot \pi \cdot \rho}{L}\right) - b_n \cdot K1\left(\frac{n \cdot \pi \cdot \rho}{L}\right)\right) \cdot \left(\cos\left(\frac{n \cdot \pi \cdot z}{L}\right) - 1\right)$$

The radial distortion integral is shown as a function of z for paths at several different radii in Figure 17

$k := 0 .. 7$

$\rho_k := 55 \cdot cm + k \cdot 20 \cdot cm$

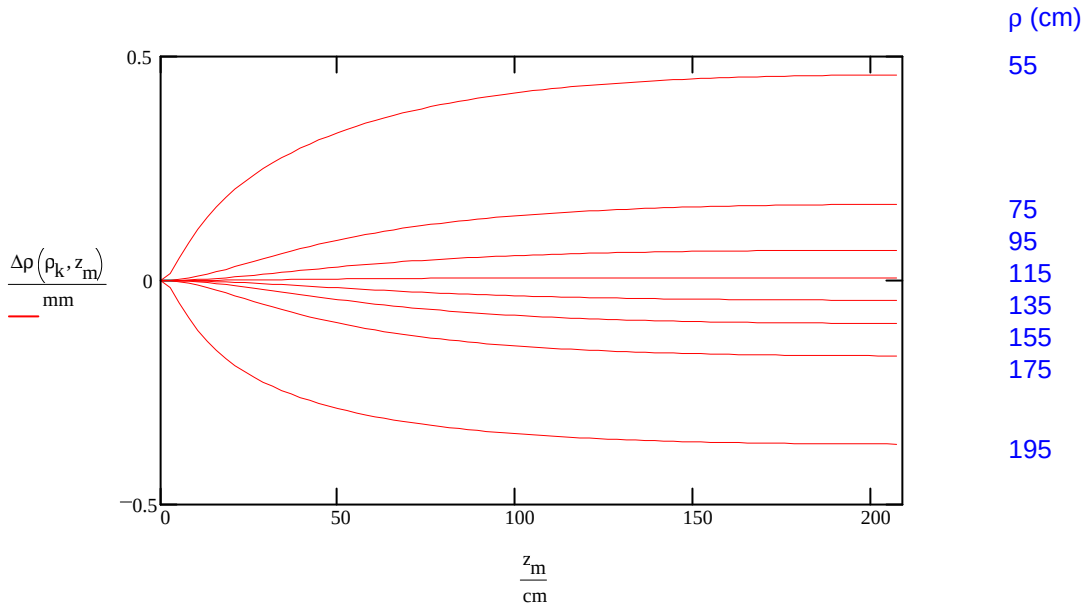

Figure 17. The radial distortion integral is shown as a function of z for equally spaced radial paths starting at 55 cm (5 cm from the inner cylinder) and ending at 195 cm (5 cm from the other field cage cylinder. This is the distortion resulting from a voltage mismatch at end ground plane electrode (pad plane) of 3 volts for a total 30 kV on the field cage.

The distortion shown in Figure 17 is for a 10^{-4} mismatch. This corresponds to a mismatch in the potential at the ground plane of 3 volts out of 30 kV or a mechanical misplacement in z of 0.2 mm. The voltage trimming should be reasonably easy to maintain, but this also implies a mechanical requirement of maintaining the pad plane parallel to the equipotential rings to within ~0.4 mm to maintain the 0.7 mm limit for the radial distortion integral. This will be a challenging mechanical problem.

8. Conclusion

We have developed a calculation for determining electron drift distortion for the standard concentric cylinder TPC field cage given the error potential on the cylinder walls. This method has the advantage that it is easy to input the boundary conditions and it only takes a few seconds to run. This code has been checked against a Poisson calculation done by Russ Wells [5], and the results agree to better than 5 %. The method has been used to check the effects of reduced resistance on one section of the STAR TPC field cage and shows that a distortion will exist, but it is within the design tolerance which requires that a false sagitta be less than 200 μm. We have also done

calculations for distortions due to finite width of the equipotential rings, errors in resistor chain values, effects of ordering the resistors by value, shorted resistors and voltage mismatch of the cylinder with the end planes. As expected, finite width of the equipotential rings is not a problem and if necessary we could join 5 rings together without affecting resolution as long as joined rings are maintained at the proper potential. The tolerance on resistor precision is consistent with what has been done in the past as long as the resistors are not sorted by value along the z. This ordering can increase the error over random placement or high-low pairing by a factor of 5 to 10. A shorted stripe pair in the field cage has a characteristic large distortion that should be easy to recognize and if necessary a calculated correction could be applied. However, a factor of 10 correction would be required to maintain the desired 0.7 mm radial distortion integral limit. Doug Greiner has pointed out that a simple fix for shorted stripes could be accomplished by simply changing the divider resistors on either side of the shorted section[6]. The final distortion studied in this note addresses proper matching of the field cage cylinder ground end voltage with the pad plane. Proper matching will require trimming the voltage to within 6 volts of nominal when operating with a terminal voltage of 30 kV. This will not be as difficult as maintaining the mechanical matching of 0.4 mm.

Appendix 1

Derivation of the Radial Distortion Formula

The derivation of the formula for the drift distortion integral:

$$\Delta\rho(\rho,z)=\int_{z}^{0}\frac{E_\rho(\rho,z)}{E_z}\,dz \qquad \text{A1(1)}$$

is developed from section 3.6, "Laplace Equation in Cylindrical Coordinates, Bessel Functions" of Jackson[3]. We calculate the case for a volume (see Figure 1) defined by two concentric cylinders closed at the ends with planes perpendicular to the axis. The potential on the ends is 0 and the potential on the two cylinders can be given any function of z that goes to 0 at the two ends and is rotationally invariant.

The first step is to write down the solution to Laplace's equation for the error potential. Laplace's equation with the separation of variables (there is no ϕ dependence in this problem)

$$\Phi(\rho,z)=R(\rho)\cdot Z(z) \qquad \text{A1(2)}$$

is

$$\frac{d^2}{d\rho^2}R+\frac{1}{\rho}\cdot\frac{d}{d\rho}R-k^2\cdot R=0 \qquad \text{A1(3)}$$

and

$$\frac{d^2}{dz^2}Z+k^2\cdot Z=0 \qquad \text{A1(4)}$$

We have chosen the sign of the coupling constant, k^2, given at the end of Jackson's[2] section 3.6. This gives the Z equation, A1(4) which has a solution of

$\sin(kz)$ or $\cos(kz)$

This can be used in an expansion of the potential along the inner and outer cylinders. Since the potential must go to 0 at the ends, z=0 and z=L, then the sine function is the appropriate solution and the coupling constant, k, must be limited to

$$k=\frac{n\cdot\pi}{L}$$ where n is an integer. A1(5)

The linearly independent solutions to the radial equation, A1(3), are the zeroth order modified Bessel functions of the first and second kind,

$$I0\left(\frac{n\cdot\pi\cdot\rho}{L}\right)$$

and

$$K0\left(\frac{n\cdot\pi\cdot\rho}{L}\right)$$

respectively, where the restricted value of k has been included.

The combined solution is:

$$\Phi(\rho,z)=\sum_{n=1}^{\infty}\left(A_n\cdot I0\left(\frac{n\cdot\pi\cdot\rho}{L}\right)+B_n\cdot K0\left(\frac{n\cdot\pi\cdot\rho}{L}\right)\right)\cdot\sin\left(\frac{n\cdot\pi\cdot z}{L}\right) \qquad \text{A1(6)}$$

The coefficients A_n and B_n are evaluated using the potentials given on the inner and outer cylinders in the following manner:

$$\int_0^L \Phi(\rho ir,z)\cdot\sin\left(\frac{n\cdot\pi\cdot z}{L}\right)dz=\left(A_n\cdot I0\left(\frac{n\cdot\pi\cdot\rho ir}{L}\right)+B_n\cdot K0\left(\frac{n\cdot\pi\cdot\rho ir}{L}\right)\right)\cdot\frac{L}{2} \qquad \text{A1(7)}$$

and

$$\int_0^L \Phi(\rho or,z)\cdot\sin\left(\frac{n\cdot\pi\cdot z}{L}\right)dz=\left(A_n\cdot I0\left(\frac{n\cdot\pi\cdot\rho or}{L}\right)+B_n\cdot K0\left(\frac{n\cdot\pi\cdot\rho or}{L}\right)\right)\cdot\frac{L}{2} \qquad \text{A1(8)}$$

since $$\int_0^L \sin\left(\frac{np\cdot\pi\cdot z}{L}\right)\cdot\sin\left(\frac{n\cdot\pi\cdot z}{L}\right)dz=\frac{L}{2}\cdot\delta_{np,n}$$

ρir inner cylinder radius

ρor outer cylinder radius

The equations A1(7) and A1(8) are a pair of linear equations which can be solved for A_n and B_n giving

$$A_n = \frac{Sir_n \cdot K0\left(\frac{n\cdot\pi\cdot\rho or}{L}\right) - Sor_n \cdot K0\left(\frac{n\cdot\pi\cdot\rho ir}{L}\right)}{I0\left(\frac{n\cdot\pi\cdot\rho ir}{L}\right)\cdot K0\left(\frac{n\cdot\pi\cdot\rho or}{L}\right) - I0\left(\frac{n\cdot\pi\cdot\rho or}{L}\right)\cdot K0\left(\frac{n\cdot\pi\cdot\rho ir}{L}\right)} \qquad \text{A1(9)}$$

$$B_n = \frac{Sor_n \cdot I0\left(\frac{n\cdot\pi\cdot\rho ir}{R}\right) - Sir_n \cdot I0\left(\frac{n\cdot\pi\cdot\rho or}{L}\right)}{I0\left(\frac{n\cdot\pi\cdot\rho ir}{L}\right)\cdot K0\left(\frac{n\cdot\pi\cdot\rho or}{L}\right) - I0\left(\frac{n\cdot\pi\cdot\rho or}{L}\right)\cdot K0\left(\frac{n\cdot\pi\cdot\rho ir}{L}\right)} \qquad \text{A1(10)}$$

where

$$Sir_n = \frac{2}{L}\cdot\int_0^L \Phi(\rho ir, z)\cdot\sin\left(\frac{n\cdot\pi\cdot z}{L}\right) dz \qquad \text{A1(11)}$$

and

$$Sor_n = \frac{2}{L}\cdot\int_0^L \Phi(\rho or, z)\cdot\sin\left(\frac{n\cdot\pi\cdot z}{L}\right) dz \qquad \text{A1(12)}$$

Note that in the solution for a simple cylinder (no inner cylinder boundary) where the potential is finite at $\rho = 0$ there can be no K0 function so $B_n = 0$ and A_n is given by equation A1(8).

Having an expression for the potential (Eq. A1(6)) and a way of determining the coefficients, we are ready to determine the radial distortion (Eq. A1(1)), but first it is slightly simpler to switch to a normalized error potential, i.e.:

$\phi(\rho, z)$ where $\Phi(\rho, z) = V\cdot\phi(\rho, z)$ A1(13)

V is the full voltage on the field cage generating the drift field. This voltage appears in the radial distortion expression in terms of the drift field E_z, namely:

$$E_z = \frac{V}{L}$$ A1(14)

Changing to the normalized potential Eq. A1(6) and Eqs. A1(9) - A1(12) become:

$$\Phi(\rho, z) = V \cdot \sum_{n=1}^{\infty} \left(a_n \cdot I0\left(\frac{n \cdot \pi \cdot \rho}{L}\right) + b_n \cdot K0\left(\frac{n \cdot \pi \cdot \rho}{L}\right) \right) \cdot \sin\left(\frac{n \cdot \pi \cdot z}{L}\right)$$ A1(15)

$$a_n = \frac{sir_n \cdot K0\left(\frac{n \cdot \pi \cdot \rho or}{L}\right) - sor_n \cdot K0\left(\frac{n \cdot \pi \cdot \rho ir}{L}\right)}{I0\left(\frac{n \cdot \pi \cdot \rho ir}{L}\right) \cdot K0\left(\frac{n \cdot \pi \cdot \rho or}{L}\right) - I0\left(\frac{n \cdot \pi \cdot \rho or}{L}\right) \cdot K0\left(\frac{n \cdot \pi \cdot \rho ir}{L}\right)}$$ A1(16)

$$b_n = \frac{sor_n \cdot I0\left(\frac{n \cdot \pi \cdot \rho ir}{R}\right) - sir_n \cdot I0\left(\frac{n \cdot \pi \cdot \rho or}{L}\right)}{I0\left(\frac{n \cdot \pi \cdot \rho ir}{L}\right) \cdot K0\left(\frac{n \cdot \pi \cdot \rho or}{L}\right) - I0\left(\frac{n \cdot \pi \cdot \rho or}{L}\right) \cdot K0\left(\frac{n \cdot \pi \cdot \rho ir}{L}\right)}$$ A1(17)

$$sir_n = \frac{2}{L} \cdot \int_0^L \phi(\rho ir, z) \cdot \sin\left(\frac{n \cdot \pi \cdot z}{L}\right) dz$$ A1(18)

$$sor_n = \frac{2}{L} \cdot \int_0^L \phi(\rho or, z) \cdot \sin\left(\frac{n \cdot \pi \cdot z}{L}\right) dz$$ A1(19)

In the radial distortion expression, Eq. A1(1)

$$E_\rho(\rho, z) = \frac{d}{d\rho} \Phi(\rho, z)$$ A1(20)

Using Eq. A1(15) for Φ and the derivative relations:

$$\frac{d}{dx}I0(x)=I1(x) \quad \text{and} \quad \frac{d}{dx}K0(x)=-K1(x) \qquad \text{A1(21)}$$

$$E_\rho(\rho,x)=V\cdot\sum_{n=1}^{\infty}\frac{n\cdot\pi\cdot\rho}{L}\cdot\left(a_n\cdot I1\left(\frac{n\cdot\pi\cdot\rho}{L}\right)-b_n\cdot K1\left(\frac{n\cdot\pi\cdot\rho}{L}\right)\right)\cdot\sin\left(\frac{n\cdot\pi\cdot z}{L}\right) \qquad \text{A1(22)}$$

where I1 and K1 are the first order modified Bessel functions of the first and second kind.

The derivatives, A1(21), can be obtained using expressions 3.87 and 3.88 of Jackson[3].

To get the final result, substitute the expressions A1(22) for E_ρ and A1(14) for E_z into

$$\Delta\rho(\rho,z)=\int_z^0\frac{E_\rho(\rho,z)}{E_z}\,dz$$

and perform the integration to get:

$$\Delta\rho(\rho,z)=L\cdot\sum_{n=1}^{\infty}\left(a_n\cdot I1\left(\frac{n\cdot\pi\cdot\rho}{L}\right)-b_n\cdot K1\left(\frac{n\cdot\pi\cdot\rho}{L}\right)\right)\cdot\left(\cos\left(\frac{n\cdot\pi\cdot z}{L}\right)-1\right) \qquad \text{A1(23)}$$

Again the coefficients are given by equations, A1(16) - A1(19)

References and footnotes:

1. W. Blum and L. Rolandi, "Particle Detection with Drift Chambers" Springer-Verlag, 1993.

2. H. Wieman, "E and B field Precision Constraints from Momentum Resolution Requirements in the STAR TPC", STAR TPC Note # 14, Oct. 91.

3. J.D. Jackson, "Classical Electrodynamics" John Wiley and Sons, Inc. 1962,1975

4. This problem could probably be solved equally well by fixing the potentials on the cylinders at 0 and defining the error potential on the end cap. The appropriate expansion is close to an example in Jackson[3], section 3.7. It should be possible to do the problem with the potential vanishing on both the inner and outer cylinder boundary by including both linear independent Bessel functions in the expansion. This approach might have application in solving the problem where the effective ground planes of the inner and outer sectors of the STAR TPC are incorrectly matched.

5. Russ Wells, private communication

6. Doug Greiner, private communication